

ENVIRONMENTAL RESEARCH  
LETTERS

## LETTER

## From trees to rain: enhancement of cloud glaciation and precipitation by pollen

## OPEN ACCESS

## RECEIVED

24 April 2024

## REVISED

23 August 2024

## ACCEPTED FOR PUBLICATION

28 August 2024

## PUBLISHED

9 September 2024

Original Content from this work may be used under the terms of the [Creative Commons Attribution 4.0 licence](#).

Any further distribution of this work must maintain attribution to the author(s) and the title of the work, journal citation and DOI.

Jan Kretzschmar<sup>1,\*</sup> , Mira Pöhlker<sup>1,2</sup> , Frank Stratmann<sup>2</sup> , Heike Wex<sup>2</sup> , Christian Wirth<sup>3,4</sup> and Johannes Quaas<sup>1,3</sup> <sup>1</sup> Leipzig University, Institute for Meteorology, Stephanstr. 3, 04103 Leipzig, Germany<sup>2</sup> Leibniz-Institute for Tropospheric Research, Permoser Str. 15, 04318 Leipzig, Germany<sup>3</sup> German Centre for Integrative Biodiversity Research (iDiv) Halle-Jena-Leipzig, Puschstr. 4, 04103 Leipzig, Germany<sup>4</sup> Max-Planck-Institute for Biogeochemistry, Hans-Knöll-Str. 10, 07745 Jena, Germany

\* Author to whom any correspondence should be addressed.

E-mail: [jan.kretzschmar@uni-leipzig.de](mailto:jan.kretzschmar@uni-leipzig.de)**Keywords:** pollen, ice nucleating particles, cloud ice fraction, precipitationSupplementary material for this article is available [online](#)**Abstract**

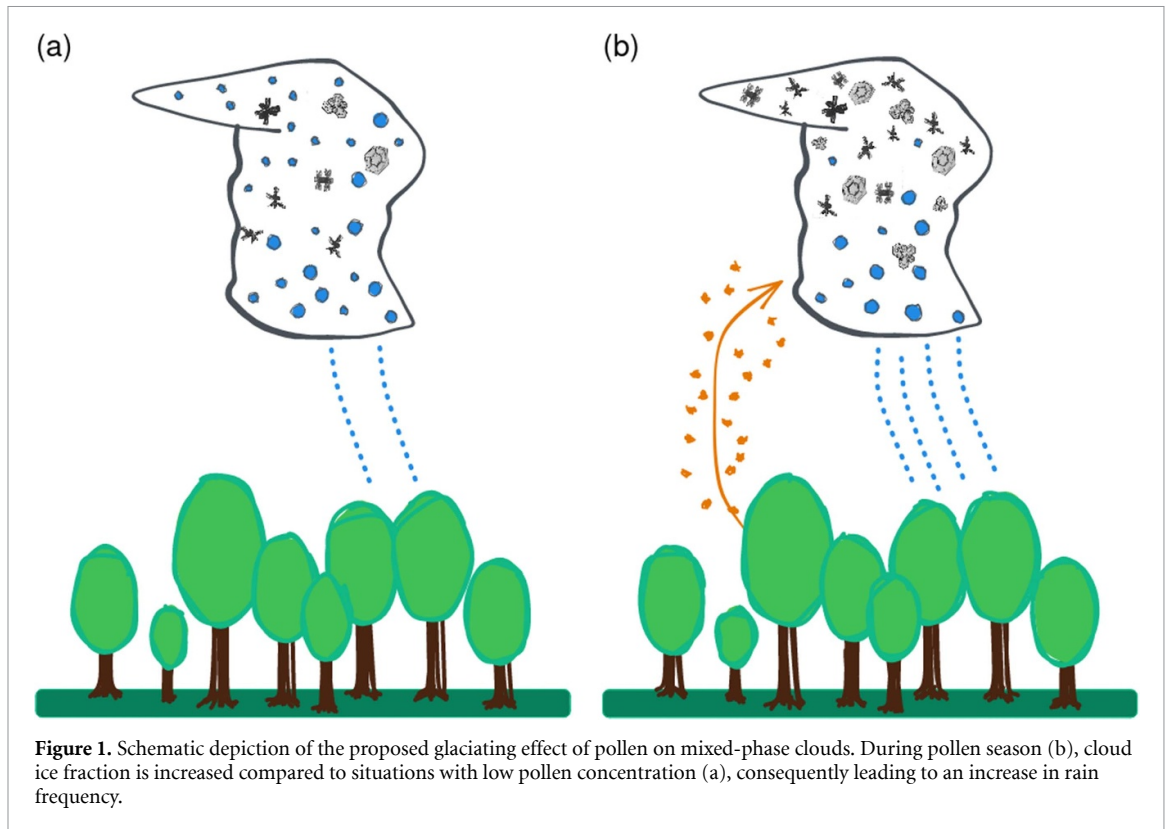
The ability of pollen to enable the glaciation of supercooled liquid water has been demonstrated in laboratory studies; however, the potential large-scale effect of plants and pollen on clouds, precipitation and climate is pressing knowledge to better understand and project clouds in the current and future climate. Combining ground-based measurements of pollen concentrations and satellite observations of cloud properties within the United States, we show that enhanced pollen concentrations during springtime lead to an increase in cloud ice fraction of up to 0.1 in the temperature regime where pollen are considered to act as INP ( $-15^{\circ}\text{C}$  and  $-25^{\circ}\text{C}$ ). We further establish the link from the pollen-induced increase in cloud ice to a higher precipitation frequency. In light of anthropogenic climate change, the extended and strengthened pollen season and future alterations in biodiversity can introduce a localized climate forcing and a modification of the precipitation frequency and intensity.

**1. Introduction**

In the absence of so-called ice nucleating particles (INP), a subset of atmospheric aerosol particles, the freezing of a liquid water droplet requires extremely low temperatures ( $-38^{\circ}\text{C}$  and colder) to overcome the energetic barrier required for so-called homogeneous nucleation. Whether or not cloud droplets glaciate for temperatures greater than  $-38^{\circ}\text{C}$  depends on the availability of the above-mentioned INP, which enable the freezing of supercooled liquid droplets or haze particles via heterogeneous freezing mechanisms at temperatures between  $0^{\circ}\text{C}$  and  $-38^{\circ}\text{C}$ . The thermodynamic state of clouds is of particular importance for their propensity to form rain. The vast majority of rain events over the continents and outside tropical and sub-tropical oceans originate from ice clouds (Field and Heymsfield 2015, Mülmenstädt *et al* 2015). It has been demonstrated that pollen are among the aerosol species that may serve as INP (Diehl *et al* 2001, 2002, von Blohn *et al* 2005, Pummer

*et al* 2012, Augustin *et al* 2013, Hader *et al* 2014). While the contribution of pollen to the glaciation of mixed-phase clouds is thought to be rather small on a global scale compared to other INP such as dust, they can nevertheless play an important role on regional and seasonal scales (Després *et al* 2012, Pummer *et al* 2012).

Laboratory studies, investigating the freezing temperature of supercooled water droplets with embedded pollen grains indicate that most pollen induce freezing in a temperature range between  $-15^{\circ}\text{C}$  and  $-25^{\circ}\text{C}$  (see table 1 in Gute and Abbatt 2020, for a summary of laboratory studies of freezing properties of different pollen taxa). Besides the whole pollen grains, it has been shown that the so-called pollen-washing water has ice nucleating properties (Pummer *et al* 2012), where pollen grains have been filtered out from the water droplets. The ice nucleating properties of pollen washing water have been attributed to ice nucleating molecules like polysaccharides (Dreischmeier *et al* 2017), located on



the surface and within pollen grains, that act as INP (e.g. Pummer *et al* 2012, Augustin *et al* 2013, Wozniak *et al* 2018, Burkart *et al* 2021, Mikhailov *et al* 2021, Kinney *et al* 2024).

To act as INP, pollen have to first be vertically transported into sufficiently cold temperature regimes. Ground-based lidar observations have revealed that layers containing pollen can indeed reach those temperature regimes, likely being lifted to those altitudes by vertical mixing due to convection and turbulence, or due to large-scale uplift (Bohlmann *et al* 2021). Due to their relatively large size, whole pollen grains have a limited residence time in the atmosphere before they are removed by gravitational settling (Phillips *et al* 2008, Steiner *et al* 2015). This highlights the importance of so-called subpollen particles. Under humid conditions, pollen grains rupture into these subpollen particles, containing the above-mentioned ice nucleating molecules. Due to their smaller size, these subpollen particles have a longer residence time in the atmosphere and can reach higher altitudes than a whole pollen grain, increasing their ability to act as INP in the mixed-phase temperature regime (Pummer *et al* 2012, Steiner *et al* 2015, Burkart *et al* 2021, Seifried *et al* 2021). The importance of subpollen particles has further been highlighted in several modelling studies investigating the effect of pollen on cloud microphysics (e.g. Wozniak and Steiner 2017, Subba *et al* 2021, Prank *et al* 2024, Zhang *et al* 2024).

While the ice activity of pollen is widely researched in laboratory studies, so far there is no evidence on the role of pollen for cloud glaciation from observations at a large scale. In this study, we, therefore, aim at assessing whether the effect of pollen on the cloud ice fraction in the heterogeneous freezing temperature regime can be quantified using ground-based pollen concentration and satellite observations of clouds over the continental United States. We further investigate whether the enhanced freezing efficiency in the mixed-phase temperature regime induces an increased precipitation frequency as illustrated in figure 1.

## 2. Data and methods

We employ ground-based pollen concentration data collected from stations within the United States (US; the location of pollen stations used is given in figure S1). Pollen station data are disseminated by the National Allergy Bureau (NAB), which is part of the American Academy of Allergy, Asthma and Immunology (AAAAI). In this study, we use pollen concentrations collected by more than 50 surface stations in a period from 2007 to 2017. Each timeseries at a station contains pollen concentrations of up to 40 different pollen taxa, but due to a strong temporal correlation in pollen emission, we simplify the analysis by only using total pollen concentration in our analysis. We need to remark that not all stations cover

the full time period of interest, but cloud properties in the vicinity of a pollen station are only sampled if information on pollen concentration is available. We chose a radius of 100 km around a pollen station within which we sample cloud properties from satellite products. The composition of pollen-emitting plants (see figure 1 in Watson *et al* 2015) and climatic conditions in the continental US are rather homogeneous. Under such conditions, Nowosad *et al* (2015) has shown that pollen emission can be considered to be spatiotemporally homogeneous. We nevertheless do not want to overextend this assumption, as long-range transport clearly has been shown to decorrelate observed pollen concentrations from local emissions (e.g. Sofiev 2017). For that reason, we evaluated the effect of using different sampling radii around the pollen stations for cloud properties from the satellites, but the findings in this study were independent of the employed sampling radius.

We use daily data from the Moderate Resolution Imaging Spectroradiometer (MODIS) Level-2, Collection 6.1 dataset at a horizontal resolution of 1 km, from both, the Aqua and Terra satellite. Due to the wide swath of MODIS, a large number of satellite pixels are available in the vicinity of a pollen station, which enables us to calculate cloud ice fraction  $f_i$  as a function of temperature at each station and timestep. An evaluation of the employed MODIS retrieval algorithm for cloud phase shows good agreement with cloud phase derived from the spaceborne CALIPSO lidar (Marchant *et al* 2016), providing confidence in the retrieved ice fraction. Comparisons of retrieved cloud-top height from MODIS to cloud-top height from active satellite remote sensing have highlighted that differences of a few hundred meters are present (e.g. Håkansson *et al* 2018, Mitra *et al* 2021) for clouds below 5 km. Both Håkansson *et al* (2018) and Mitra *et al* (2021) showed that the sign of the bias is furthermore dependent on cloud optical thickness, where cloud top height in MODIS was underestimated for optically thick clouds while being overestimated for optically thin clouds. As these biases will similarly affect clouds sampled for low and high pollen concentrations, we do not expect major inconsistencies in the comparison of cloud ice fraction as a function of cloud top temperature.

At each cloudy satellite pixel, the MODIS cloud phase retrieval indicates if a cloud is liquid or ice, or if the cloud phase retrieval is uncertain. Due to the fact that the cloud phase retrieval in the MODIS dataset is dependent on information from shortwave spectral bands, we only use daytime overpasses in our analysis. Furthermore, we only consider pixels that are flagged as single-layer clouds by the MODIS retrieval to avoid uncertain retrievals in cloud top temperature and phase. From the ratio of pixels in the ice phase to the total number of cloudy pixels within the 100 km sampling radius, we calculate  $f_i$ , binned by cloud top

temperature at each station ( $s$ ) and each satellite overpass/timesteps ( $t$ ), defined as:

$$f_i(T, s, t) = \frac{n_{\text{ice}}(T, s, t)}{\sum_j n_j(T, s, t)} \quad j \in \{\text{ice, liquid, undetermined}\}. \quad (1)$$

Here we use a bin width of 2 K between  $-50^\circ\text{C}$  and  $10^\circ\text{C}$ . To compare high and low pollen cases, we calculate the mean of  $f_i$  at each temperature bin among all stations and timesteps, respectively. Here, a weighted mean is employed to give more weight to situations having more cloudy pixels within the sampling radius, such that:

$$\bar{f}_i(T) = \frac{\sum_{s,t} w(T, s, t) f_i(T, s, t)}{\sum_{j,s,t} n_j(T, s, t)} \quad \text{with } w(T, s, t) = \sum_j n_j(T, s, t). \quad (2)$$

To quantify statistical uncertainty in the difference of  $\bar{f}_i(T)$  between high and low pollen cases, we bootstrapped the mean of high and low pollen cases using a sample size of 10 000 to calculate the 95% confidence interval for this difference.

We additionally use information on cloud properties from DARDAR (raDAR/liDAR, Delanoë and Hogan 2010), combining data from a spaceborne cloud radar (CloudSat; Stephens *et al* 2002) and cloud lidar (CALIPSO; Winker *et al* 2003). In particular, we use information from the so-called DARDAR\_MASK, which contains information on atmospheric features like the phase state of clouds, precipitation and atmospheric aerosols. The fact that information on atmospheric features are sampled along the ground track of the two satellites drastically limits the number of available data points in the vicinity of a pollen station. For that reason, we only look at the entire spring-time period (MAM), increased the sampling radius to 200 km, and additionally increased the width of the temperature bins to 10 K. As DARDAR employs information from active sensors that are independent of insolation, we additionally use nighttime overpasses to increase the number of available overpasses over pollen stations.

To be comparable to MODIS, we first have to detect cloud top in the DARDAR dataset. To avoid spurious detection of a cloud layer in DARDAR, at least four consecutive cloudy points within each vertical profile (which is equivalent to a geometrical cloud depth of at least 240 m) have to be present. The cloud phase at cloud top is then considered in the ice fraction calculation. We only use situations where one cloud top is detected in DARDAR to be comparable to MODIS data, where we also consider only single-layer clouds. While MODIS actually infers cloud top temperature from observed radiances, cloud top temperature in DARDAR is derived from ECMWF-AUX,

the spatially interpolated meteorological analysis of the European Centre for Medium-Range Weather Prediction (ECMWF). MODIS only distinguishes between liquid and ice clouds, whereas in DARDAR also mixed-phase clouds (ice+supercooled) can be detected, which we consider to be in the liquid phase. In contrast to the MODIS analysis, we do not calculate ice fraction for a single pollen station which was subsequently averaged across all pollen stations, due to the limited amount of data points along the satellite ground track in the vicinity of pollen stations. For that reason, we combine information on cloud phase from all overpasses over pollen stations and calculate  $\bar{f}_i$  as follows:

$$\bar{f}_i(T) = \frac{n_{\text{ice}}(T)}{\sum_j n_j(T)} \quad j \in \{\text{ice, mixed phase, supercooled, liquid}\}, \quad (3)$$

where  $n_j$  is the number of pixels of the respective cloud phase category.

Using the ability of DARDAR to penetrate through optically thick clouds and to retrieve information on cloud and hydrometeor properties almost down to the surface, we are furthermore able to assess whether an effect of pollen on precipitation can be identified. We quantify this by comparing the fraction of precipitating clouds for high and low pollen situations. As information on whether a cloud is precipitating is derived from CloudSat, which suffers from ground clutter, we assume a cloud to be precipitating when the DARDAR\_MASK profile indicates precipitation at 500 m above ground level. Using this information, we calculate the ratio of precipitating clouds  $\bar{f}_p$  for temperatures between  $-50^\circ\text{C}$  to  $10^\circ\text{C}$ . Besides the directly derived fraction of precipitating clouds, we recalculate this value from changes in ice fraction, enabling us to quantify the effect of modified ice fraction on precipitation when pollen are present. Any deviation for the directly calculated precipitation fraction is indicative of other processes that influence rain fraction besides the glaciating effect of pollen. The total fraction of precipitating clouds can then be calculated as follows:

$$f_p(T) = \bar{f}_i(T) p_{\text{ice}}(T) + [1 - \bar{f}_i(T)] p_{\text{liq}}(T), \quad (4)$$

where  $p_{\text{ice}}(T)/p_{\text{liq}}(T)$  is the fraction of ice/liquid clouds that precipitate at a temperature bin, which we calculated from all available DARDAR profiles in the USA from 2007 to 2016. We again employ a weighted mean to calculate the mean fraction of precipitating clouds for all temperature bins from  $-50^\circ\text{C}$  to  $10^\circ\text{C}$ :

$$\bar{f}_{p,\text{calc}} = \sum_T w(T) f_p(T) \quad (5)$$

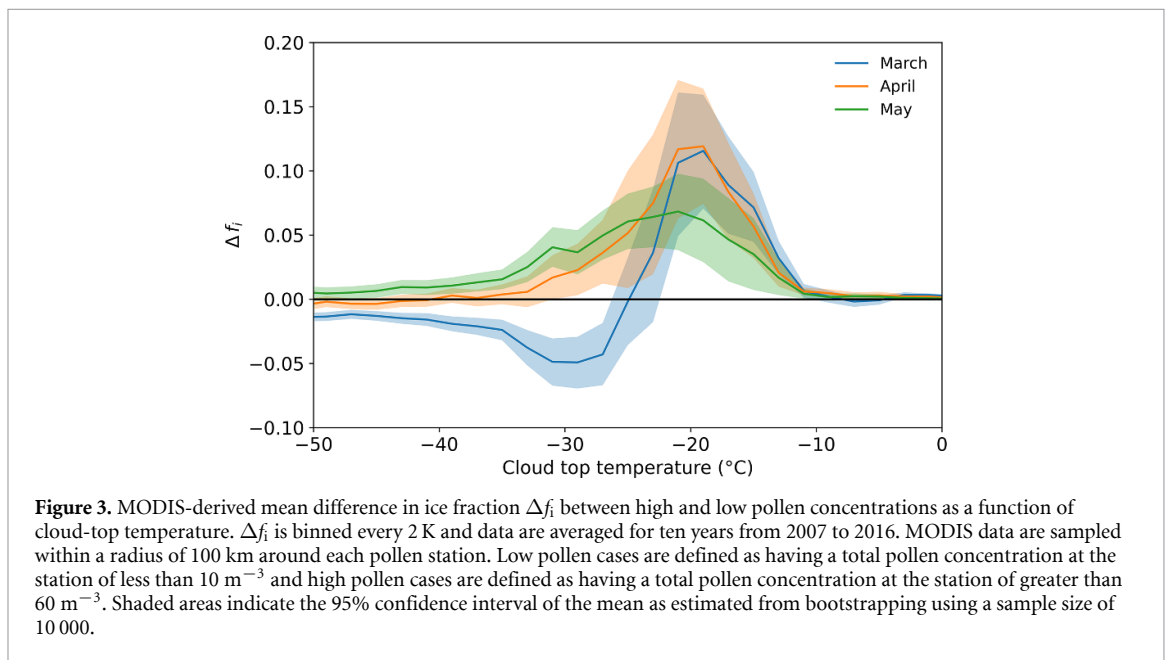
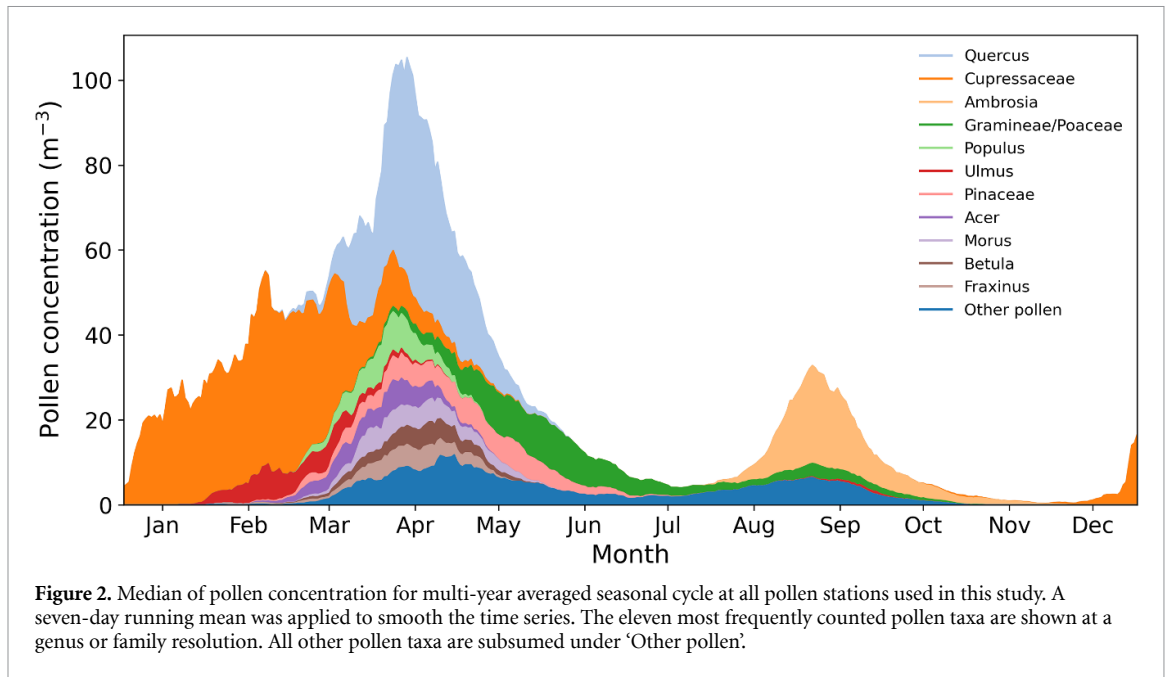
where  $w(T)$  is the ratio of cloudy profiles to the number of cloudy profiles in that temperature bin.

### 3. Results

As a proxy for pollen concentration in the atmosphere, we employ ground-based pollen concentration observations, collected from stations within the United States (US; the location of pollen stations used is given in figure S1). Wozniak and Steiner (2017) showed that two distinct maxima in pollen concentration can be identified in the US, one during spring and one in fall, which can be consistently identified across all regions of the US. In the following, we will focus on the springtime (March–April–May, MAM) maximum, to which mostly deciduous broadleaf trees and Cupressaceae contribute. As shown in figure 2, the emission of different pollen taxa in this period is strongly temporally correlated, making it difficult to disentangle the effect of a single pollen taxon. Therefore, we decided to simplify our analysis by only using the total pollen concentration observed at the respective stations as a proxy for pollen concentration in the atmosphere. In the following, we compare cloud properties between high and low pollen conditions. Low pollen conditions are defined as situations where pollen concentration (grains per  $\text{m}^{-3}$ ), as measured at the surface, is less than  $10\text{m}^{-3}$ , whereas pollen concentration is considered to be high when pollen concentrations of larger than  $60\text{m}^{-3}$  are observed. The upper threshold of  $60\text{m}^{-3}$  is representative of the mean in total pollen concentration during MAM in the USA (see figure 2).

Figure 3 shows the mean difference in ice fraction as diagnosed from the MODIS dataset for cases with high and low pollen concentrations. We find a maximum in the difference between high and low pollen conditions at around  $-20^\circ\text{C}$ , which is most strongly expressed in March and April and is slightly reduced in May. For all months, the positive difference in ice fraction is statistically significant for a cloud top temperature range between  $-17^\circ\text{C}$  and  $-23^\circ\text{C}$ . This increased ice fraction is in good agreement with the freezing temperature of water-embedded pollen grains/pollen-washing water between  $-15^\circ\text{C}$  and  $-25^\circ\text{C}$ , reported in laboratory studies (Gute and Abbatt 2020). We would like to remark that for temperatures greater than  $-13^\circ\text{C}$ , the cloud phase retrieval of MODIS gives large weight towards the liquid phase (supplemental material in Platnick *et al* 2017), so the difference between high and low pollen concentrations is close to zero in that temperature regime.

To further constrain the influence of pollen on cloud ice fraction, we subdivided the continental US into three sub-regions (western, southeastern, and northeastern US; figure S1). When focusing on the



two regions in the eastern US, we find a temporal variation in the response of cloud ice fraction to pollen concentration. The largest difference in ice fraction for the southeastern US is observed already in March, whereas the suspected effect of pollen on ice fraction only can be seen for April and May in the northeastern US. This delayed response in ice fraction coincides with the later start of the pollen season in higher latitudes (Lo *et al* 2019), strengthening the causal relationship between the presence of pollen and the increased cloud ice fraction.

As meteorological conditions strongly change during springtime, we evaluated whether the above-reported signal in ice fraction might stem from a temporal covariability of pollen and meteorology. We

first evaluated whether there is a general temporal trend in cloud ice fraction during springtime by comparing the beginning to the end of all springtime months. We find that cloud ice fraction decreases during each month in the mixed-phase cloud temperature regime (see figure S2). From figure 2 we see that pollen concentration on US average is increasing in March, rather constant in April and decreasing in May. The fact that there is a temporal trend of pollen concentration in some months implies that filtering for low or high pollen concentration will lead to an implicit temporal sampling. For example, low pollen concentration occur in the beginning and high pollen concentration occur during the end of March. In combination with the observed decreases



**Table 1.** Relative difference between high and low pollen concentrations in column load for aerosol types in the CAMS aerosol reanalysis.

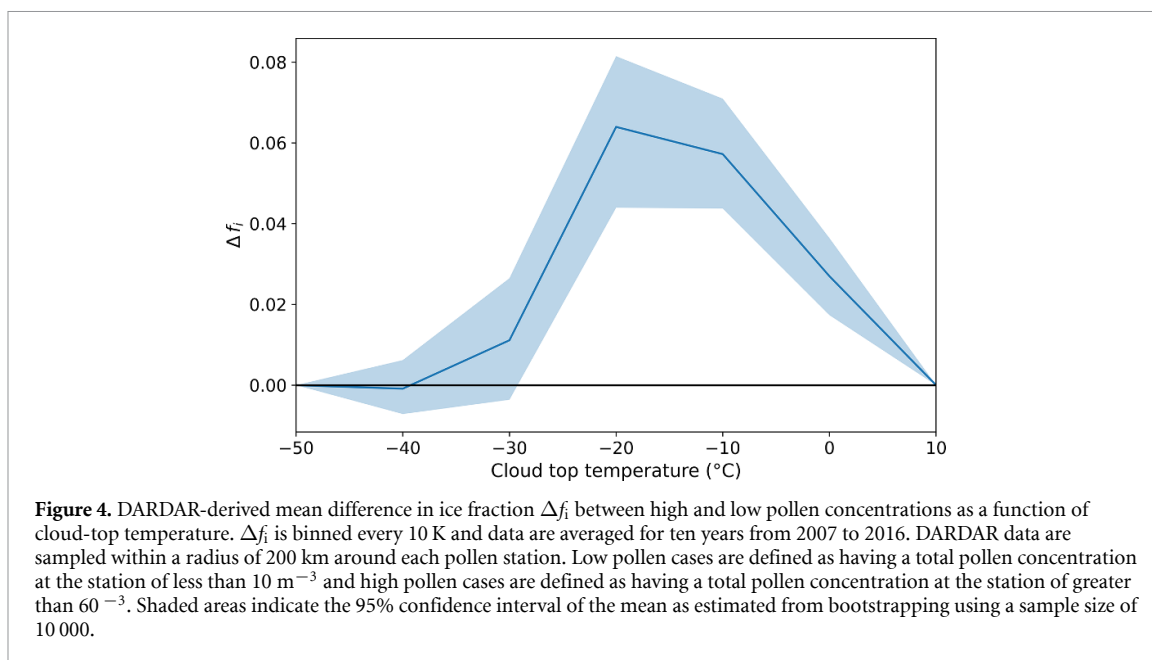
| $\Delta_{\text{rel}}$<br>(high—low pollen) | March (%) | April (%) | May (%) |
|--|-----------|-----------|---------|
| Black carbon<br>(hydrophilic)              | 8.0       | 0.8       | −1.7    |
| Organic<br>matter<br>(hydrophilic)         | 15.0      | 3.1       | −6.9    |
| Black carbon<br>(hydrophobic)              | −0.8      | −2.0      | 5.7     |
| Organic<br>matter<br>(hydrophobic)         | 4.3       | −1.8      | 1.2     |
| Sulphate                                   | −7.3      | −2.6      | 3.0     |
| Dust                                       | −26.6     | −13.3     | 12.2    |
| Sea salt                                   | −6.8      | 3.5       | 14.2    |

in ice fraction during March, this implicit temporal sampling contributes to the negative cloud ice fraction differences in March for temperatures less than  $-25^{\circ}\text{C}$ . For that reason, the signal of pollen at temperatures less than  $-25^{\circ}\text{C}$  in March would be comparable to that in April when excluding the alteration of ice fraction due to changing meteorological conditions. The effect of implicit temporal sampling flips sign in May, as there is now a decreasing trend in pollen emission towards the end of the month, so part of the increased cloud ice fraction in figure 3 might be related to this implicit temporal sampling.

Besides pollen, other aerosol species like dust may act as INP in the temperature range where pollen are ice-active. For that reason, we further investigated whether the presence of pollen is spatiotemporally correlated with other aerosols. As there is only a limited amount of long-term observations of aerosol available in the vicinity of pollen stations, we use information on the presence of aerosol from the Copernicus Atmospheric Monitoring Service (CAMS; Inness *et al* 2019) aerosol reanalysis. CAMS is based on the European Centre for Medium-Range Weather Forecast (ECMWF) Integrated Forecast System model, which has been extended to model the emission, transport and removal of aerosols and trace gases. The modelled aerosol optical depth (AOD) in CAMS is further constrained by assimilating spaceborne observation of AOD from Envisat's Advanced Along-Track Scanning Radiometer (AATSR, 2003–2012 Popp *et al* 2016) and MODIS (2003–present; Levy *et al* 2013). CAMS has proven to perform well in comparison with ground-based observation of AOD and also in comparison with the MERRA-2 aerosol reanalysis (Gueymard and Yang 2020). In table 1, we show the relative change in aerosol column load between high and low pollen concentration for different aerosol species modelled in CAMS. We find that dust load is reduced by

up to 20% in March and April, which are the month where we found the strongest susceptibility of cloud ice fraction to pollen. Dust load in the atmosphere over continental US has a seasonal cycle with a maximum during summer. During springtime, dust load is already increasing, but as indicated in figure S2, cloud ice fraction is decreasing during springtime, so any effect of the increased dust load is more than compensated by the seasonal modification of ice fraction. As stated above, the effect of pollen on ice fraction is more than able to compensate for the seasonal alteration in ice fraction, further highlighting their strong ice nucleating properties. Other aerosol species that might act as INP like organic matter only show a rather weak correlation with pollen concentrations. In CAMS, emission sources for organic matter only include anthropogenic sources and fires (Morcrette *et al* 2009), explaining the weak correlation with pollen as they are not considered in CAMS. The fact that other aerosol species only show weak relationships with pollen is further strengthening the relationship between ice fraction and pollen concentration.

To verify the results from MODIS, we additionally employed data from active satellite remote sensing. We use DARDAR (raDAR/liDAR, Delanoë and Hogan 2010), which combines information from a spaceborne cloud radar (CloudSat; Stephens *et al* 2002) and cloud lidar (CALIPSO; Winker *et al* 2003). The difference in cloud ice fraction as a function of cloud top temperature for DARDAR is shown in figure 4. We again find an increased ice fraction which peaks at  $-20^{\circ}\text{C}$ . While the maximum is in accordance with the MODIS-derived difference in ice fraction, the DARDAR-derived positive difference in ice fraction extends towards warmer temperatures up to the freezing point. The difference to MODIS can be related to the more sensitive cloud phase retrieval of DARDAR with respect to ice clouds especially at temperatures



greater than  $-10^\circ\text{C}$ . According to laboratory studies, pollen are not considered to be strongly ice-active at such elevated temperatures, so this signal can potentially be related to aerosol species like bacteria and/or fungal spores, which are ice-active in this temperature regime (e.g. Murray *et al* 2012, Kanji *et al* 2017) or to aforementioned cross-correlation with meteorological conditions.

Using the ability of DARDAR to penetrate through optically thick clouds and to retrieve information on cloud and hydrometeor properties almost down to the surface, we can assess whether an effect of the increased ice fraction due to the presence of pollen on precipitation can be identified. As most precipitation over the continents stems from the ice phase (Mülmenstädt *et al* 2015), it is expected that the enhanced cloud ice fraction in response to a higher atmospheric pollen concentration leads to an increase in the fraction of clouds that precipitate. While for low pollen cases, the fraction of precipitating clouds is  $9.19\% \pm 0.37\%$ , it increases to  $11.82\% \pm 0.19\%$  for high pollen cases, where the given uncertainty is the 95% confidence interval of the mean derived from bootstrapping with a sample size of 10 000. We remark that not all of this increase is causally linked to the increase in ice-containing clouds. Further causes are a temporal correlation between the seasonal shift in precipitation frequency and pollen concentration as discussed for cloud ice fraction. Also, the opposite causality exists: precipitation affects pollen concentration in the atmosphere. While precipitation reduces the amount of aerosol in the atmosphere through wet deposition, it has also been demonstrated that pollen concentrations can even increase before and during rainfall events (Kluska *et al* 2020).

A reason for this is that pollen can get lifted by higher wind speeds before and during rainfall events.

To be able to directly relate alteration in cloud ice fraction between high and low pollen concentrations to alteration in precipitation frequency, we calculated how this change translates into changes in precipitation frequency, given the cloud distribution by temperature and the change in precipitation probability (see Methods). We find, as expected, a smaller effect of pollen on the fraction of precipitating clouds from  $9.53\% \pm 0.02\%$  for low pollen cases to  $10.13\% \pm 0.01\%$  for high pollen cases. This still is a substantial absolute increase of 0.6% more frequent rain due to the alteration in cloud glaciation over the continental USA during springtime.

#### 4. Conclusion

We have shown that on a regional scale, pollen can have a significant ice nucleating effect, in particular during springtime when large amounts of pollen are emitted. This is in contrast to the assumed global effect of pollen, which is thought to be low as reported by Hoose *et al* (2010) from a study with a global climate model. At the time of the study of Hoose *et al* (2010), it was not known that there are ice nucleating molecules on pollen which can cause sub-pollen particles to be ice-active. This led to an underestimation of the overall contribution of pollen to the amount of ice nucleation particles in this past study. The importance of subpollen particles has been highlighted in modelling studies, in particular their ability to act as CCN (Wozniak *et al* 2018) and INP (Subba *et al* 2021, Werchner *et al* 2022, Prank *et al*

2024, Zhang et al 2024). This underlines the importance to include effects in sub-pollen particles into climate models to correctly estimates their effect on cloud microphysics and precipitation.

Anthropogenic climate change has already been shown to shift the start of springtime pollen emissions, lengthen the pollen season and increase the concentration of airborne pollen (Ziska et al 2019, Anderegg et al 2021). These trends will continue to manifest themselves towards the end of the century due to increased temperatures, changes in precipitation amount and frequency and the fertilizing effect of a higher CO<sub>2</sub> concentration (Zhang and Steiner 2022). Our results show that those changes can, at least regionally and during springtime, have a significant effect on cloud glaciation leading to an increase in precipitation frequency. The circumstance that several plant taxa jointly produce the distinct peak in pollen production during MAM points to a potential role of biodiversity in controlling cloud glaciation and precipitation which demands further research.

### Data availability statement


The data cannot be made publicly available upon publication due to legal restrictions preventing unrestricted public distribution. The data that support the findings of this study are available upon reasonable request from the authors.

### Acknowledgments

We thank all the A A A A I National Allergy Bureau pollen station data providers. The authors thank Tom Goren for valuable discussion regarding the MODIS data. M P and J Q acknowledge funding by Horizon Europe project CleanCloud (GA 101137639).

### ORCID iDs

Jan Kretzschmar  <https://orcid.org/0000-0002-8013-5831>

Mira Pöhlker  <https://orcid.org/0000-0001-6852-0756>

Frank Stratmann  <https://orcid.org/0000-0003-1977-1158>

Heike Wex  <https://orcid.org/0000-0003-2129-9323>

Johannes Quaas  <https://orcid.org/0000-0001-7057-194X>

### References

- Anderegg W R L, Abatzoglou J T, Anderegg L D L, Bielory L, Kinney P L and Ziska L 2021 Anthropogenic climate change is worsening North American pollen seasons *Proc. Natl Acad. Sci.* **118** 1–6
- Augustin S et al 2013 Immersion freezing of birch pollen washing water *Atmos. Chem. Phys.* **13** 10989–1003
- Bohlmann S, Shang X, Vakkari V, Giannakaki E, Leskinen A, Lehtinen K E J, Päätsi S and Kompola M 2021 Lidar depolarization ratio of atmospheric pollen at multiple wavelengths *Atmos. Chem. Phys.* **21** 7083–97
- Burkart J, Gratzl J, Seifried T M, Bieber P and Grothe H 2021 Isolation of subpollen particles (SPPs) of birch: SPPs are potential carriers of ice nucleating macromolecules *Biogeosciences* **18** 5751–65
- Delanoë J and Hogan R J 2010 Combined CloudSat-CALIPSO-MODIS retrievals of the properties of ice clouds *J. Geophys. Res. Atmos.* **115** 1–17
- Després V R et al 2012 Primary biological aerosol particles in the atmosphere: a review *Tellus B* **64** 15598
- Diehl K, Matthias-Maser S, Jaenicke R and Mitra S K 2002 The ice nucleating ability of pollen: part II. Laboratory studies in immersion and contact freezing modes *Atmos. Res.* **61** 125–33
- Diehl K, Quick C, Matthias-Maser S, Mitra S K and Jaenicke R 2001 The ice nucleating ability of pollen part I: laboratory studies in deposition and condensation freezing modes *Atmos. Res.* **58** 75–87
- Dreischmeier K, Budke C, Wiehemeier L, Kottke T and Koop T 2017 Boreal pollen contain ice-nucleating as well as ice-binding ‘antifreeze’ polysaccharides *Sci. Rep.* **7** 1–13
- Field P R and Heymsfield A J 2015 Importance of snow to global precipitation *Geophys. Res. Lett.* **42** 9512–20
- Gueymard C A and Yang D 2020 Worldwide validation of CAMS and MERRA-2 reanalysis aerosol optical depth products using 15 years of aeronet observations *Atmos. Environ.* **225** 117216
- Gute E and Abbott J P D 2020 Ice nucleating behavior of different tree pollen in the immersion mode *Atmos. Environ.* **231** 117488
- Hader J D, Wright T P and Petters M D 2014 Contribution of pollen to atmospheric ice nuclei concentrations *Atmos. Chem. Phys.* **14** 5433–49
- Häkansson N, Adok C, Thoss A, Scheirer R and Hörnquist S 2018 Neural network cloud top pressure and height for MODIS *Atmos. Meas. Tech.* **11** 3177–96
- Hoose C, Kristjánsson J E, Chen J-P and Hazra A 2010 A classical-theory-based parameterization of heterogeneous ice nucleation by mineral dust, soot and biological particles in a global climate model *J. Atmos. Sci.* **67** 2483–503
- Inness A et al 2019 The CAMS reanalysis of atmospheric composition *Atmos. Chem. Phys.* **19** 3515–56
- Kanji Z A, Ladino L A, Wex H, Boose Y, Burkert-Kohn M, Cziczo D J and Krämer M 2017 Overview of ice nucleating particles *Meteorol. Monogr.* **58** 1.1–1.33
- Kinney N L H, Hepburn C A, Gibson M I, Ballesteros D and Whale T F 2024 High interspecific variability indicates pollen ice nucleators are incidental *EGU Sphere Preprint* (<https://doi.org/10.5194/bg-21-3201-2024>)
- Kluska K, Piotrowicz K and Kasprzyk I 2020 The impact of rainfall on the diurnal patterns of atmospheric pollen concentrations *Agric. For. Meteorol.* **291** 108042
- Levy R C, Mattoo S, Munchak L A, Remer L A, Sayer A M, Patadia F and Hsu N C 2013 The collection 6 MODIS aerosol products over land and ocean *Atmos. Meas. Tech.* **6** 2989–3034
- Lo F, Bitz C M, Battisti D S and Hess J J 2019 Pollen calendars and maps of allergenic pollen in North America *Aerobiologia* **35** 613–33
- Marchant B, Platnick S, Meyer K, Arnold G T and Riedi J 2016 MODIS collection 6 shortwave-derived cloud phase classification algorithm and comparisons with CALIOP *Atmos. Meas. Tech.* **9** 1587–99
- Mikhailov E F et al 2021 Water uptake of subpollen aerosol particles: hygroscopic growth, cloud condensation nuclei activation and liquid–liquid phase separation *Atmos. Chem. Phys.* **21** 6999–7022
- Mitra A, Girolamo L D, Hong Y, Zhan Y and Mueller K J 2021 Assessment and error analysis of Terra-MODIS and MISR cloud-top heights through comparison with ISS-CATS lidar *J. Geophys. Res. Atmos.* **126** e2020JD034281



- Morcrette J-J et al 2009 Aerosol analysis and forecast in the European centre for medium-range weather forecasts integrated forecast system: forward modeling *J. Geophys. Res.* **114** D06206
- Mülmenstädt J, Sourdeval O, Delanoë J and Quaas J 2015 Frequency of occurrence of rain from liquid-, mixed- and ice-phase clouds derived from a-train satellite retrievals *Geophys. Res. Lett.* **42** 6502–9
- Murray B J, O'Sullivan D, Atkinson J D and Webb M E 2012 Ice nucleation by particles immersed in supercooled cloud droplets *Chem. Soc. Rev.* **41** 6519
- Nowosad J et al 2015 Temporal and spatiotemporal autocorrelation of daily concentrations of *Alnus*, *Betula* and *Corylus* pollen in Poland *Aerobiologia* **31** 159–77
- Phillips V T J, DeMott P J and Andronache C 2008 An empirical parameterization of heterogeneous ice nucleation for multiple chemical species of aerosol *J. Atmos. Sci.* **65** 2757–83
- Platnick S et al 2017 The MODIS cloud optical and microphysical products: collection 6 updates and examples from Terra and Aqua *IEEE Trans. Geosci. Remote Sens.* **55** 502–25
- Popp T et al 2016 Development, production and evaluation of aerosol climate data records from European satellite observations *Remote Sens.* **8** 421
- Prank M, Tonntila J, Shang X, Romakkaniemi S and Raatikainen T 2024 Can pollen affect precipitation? *EGUsphere Preprint* <https://doi.org/10.5194/egusphere-2024-876> (posted online 3 May 2024, accessed 3 September 2024)
- Pummer B G, Bauer H, Bernardi J, Bleicher S and Grothe H 2012 Suspendable macromolecules are responsible for ice nucleation activity of birch and conifer pollen *Atmos. Chem. Phys.* **12** 2541–50
- Seifried T M, Bieber P, Kunert A T, Schmale D G, Whitmore K, Fröhlich-Nowoisky J and Grothe H 2021 Ice nucleation activity of alpine bioaerosol emitted in vicinity of a birch forest *Atmosphere* **12** 779
- Sofiev M 2017 On impact of transport conditions on variability of the seasonal pollen index *Aerobiologia* **33** 167–79
- Steiner A L, Brooks S D, Deng C, Thornton D C O, Pendleton M W and Bryant V 2015 Pollen as atmospheric cloud condensation nuclei *Geophys. Res. Lett.* **42** 3596–602
- Stephens G L et al 2002 The cloudsat mission and the A-Train *Bull. Am. Meteorol. Soc.* **83** 1771–90
- Subba T, Lawler M J and Steiner A L 2021 Estimation of possible primary biological particle emissions and rupture events at the Southern Great Plains ARM site *J. Geophys. Res. Atmos.* **126** e2021JD034679
- von Blohn N, Mitra S K, Diehl K and Borrmann S 2005 The ice nucleating ability of pollen: part III: new laboratory studies in immersion and contact freezing modes including more pollen types *Atmos. Res.* **78** 182–9
- Watson J V, Liang J, Tobin P C, Lei X, Rentch J S and Artis C E 2015 Large-scale forest inventories of the united states and china reveal positive effects of biodiversity on productivity *For. Ecosyst.* **2** 22
- Werchner S, Gute E, Hoese C, Kottmeier C, Pauling A, Vogel H and Vogel B 2022 When do subpollen particles become relevant for ice nucleation processes in clouds? *J. Geophys. Res. Atmos.* **127** e2021JD036340
- Winker D M, Pelon J R and McCormick M P 2003 The CALIPSO mission: spaceborne lidar for observation of aerosols and clouds *Proc. SPIE* **4893** 1–11
- Wozniak M C, Solmon F and Steiner A L 2018 Pollen rupture and its impact on precipitation in clean continental conditions *Geophys. Res. Lett.* **45** 7156–64
- Wozniak M C and Steiner A L 2017 A prognostic pollen emissions model for climate models (PECM1.0) *Geosci. Model Dev.* **10** 4105–27
- Zhang Y and Steiner A L 2022 Projected climate-driven changes in pollen emission season length and magnitude over the continental United States *Nat. Commun.* **13** 1–10
- Zhang Y, Subba T, Matthews B H, Pettersen C, Brooks S D and Steiner A L 2024 Effects of pollen on hydrometeors and precipitation in a convective system *J. Geophys. Res. Atmos.* **129** e2023JD039891
- Ziska L H et al 2019 Temperature-related changes in airborne allergenic pollen abundance and seasonality across the northern hemisphere: a retrospective data analysis *Lancet Planet. Health* **3** e124–31